defined as the parameter of ICBT in the GYN GEC ESTRO recommendation and for organs at risks (OARs) such as bladder, rectum and sigmoid colon.[13,14] HRCTV, which is a major risk for local recurrence because of residual macroscopic disease, is defined as the whole cervix and the presumed extracervical tumor extension at the time of brachytherapy. Certain dose coverage values can be defined to describe the specific shape of such a dose-volume histogram (DVH), e.g. D100 and D90, defining the minimum dose delivered to 100 and 90% of the volume of interest, respectively. The OARs were contoured using the external wall contours. Cumulative DVHs were calculated for delineated organs of bladder, rectum and sigmoid colon, and the following parameters were reported: absolute volume and minimum dose to the most irradiated 0.1, 1, 2 cm^3 (D0.1 cc, D1 cc, D2 cc, respectively).[13,14]

Dwell positions and dwell weights in the tandem, ovoids and needles were manually modified until the dose distribution was optimally matched to cover HRCTV with a 6-Gy isodose line as much as possible. This planning was com-

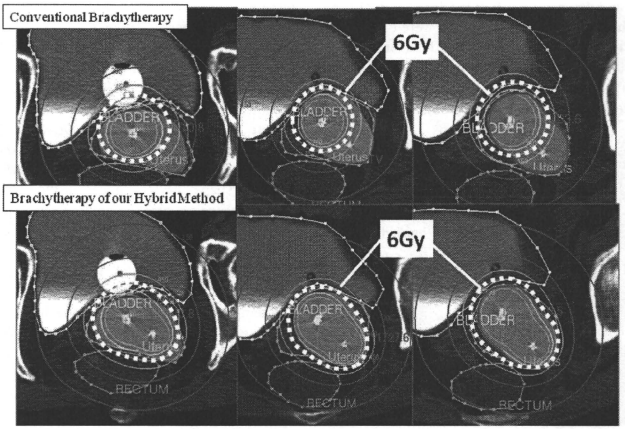

Fig. 3. Dose distribution by conventional brachytherapy and our hybrid method. : HRCTV

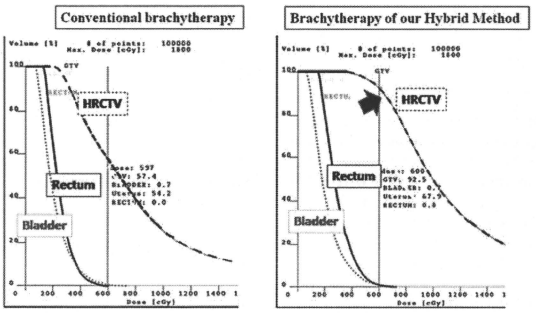

Fig. 4. Dose-Volume histograms of conventional brachytherapy planning and our hybrid method planning. — — —: HRCTV ——: Rectum ••••••••: Bladder

J. Radiat. Res. Advance Publication. This article may be modified at the final publication.

pared with conventional ICBT planning without interstitial needle by using DVH parameters for HRCTV and OARs. In conventional ICBT planning, the same source arrangement and irradiation conditions are used, and the dose distribution was based on the Manchester system. The prescribed dose was generated by the PLATO treatment planning system (TPS) with a dose of 6 Gy normalized to point A.

RESULTS

Dose distribution and dose volume histogram

Figures 3 and 4 show dose distributions and DVHs by our hybrid method and conventional ICBT. D90 to HRCTV by this hybrid method and conventional ICBT were 6.1 Gy and 3.5 Gy, respectively. D1cc of the rectum, bladder and sigmoid colon by this hybrid method were 4.8 Gy, 6.4 Gy and 3.5 Gy, respectively, whereas they were 5.7 Gy, 6.3 Gy and 3.4 Gy by conventional brachytherapy (Table 1, Fig. 4).

Table 1. Dose of HRCTV, Rectum, Bladder and Sigmoid Colon.

		Conventional brachytherapy	Our hybrid-brachytherapy
HRCTV	D100	1.9 Gy	3.4 Gy
	D90	3.5 Gy	6.1 Gy
Rectum	D0.1cc	5.8 Gy	6.7 Gy
	D1cc	4.8 Gy	5.7 Gy
	D2cc	4.4 Gy	5.2 Gy
Bladder	D0.1cc	8.0 Gy	8.0 Gy
	D1cc	6.4 Gy	6.3 Gy
	D2cc	5.8 Gy	5.8 Gy
Sigmoid colon	D0.1cc	4.5 Gy	4.3 Gy
	D1cc	3.5 Gy	3.4 Gy
	D2cc	3.2 Gy	3.2 Gy

Treatment Outcome

At 12 months after treatment, the tumor in the left parametrium had disappeared almost completely according to pelvic MRI findings. Serum levels of squamous cell carcinoma antigen and cytokeratin fragment 21-1 were reduced to 1.1 ng/ml and 3.3 ng/ml from 2.6 ng/ml and 7.6 ng/ml, respectively. No recurrent lesions and distant metastases were detected at 18 months after the treatment, and she did not experience grade 2 or higher late morbidity.

DISCUSSION

When bulky and/or irregular-shape cervical cancer is treated with brachytherapy, using increments of the prescribed dose at the reference point is one of the approaches. However, such increments may result in increasing doses to surrounding normal tissues including the bladder, rectum, and small intestine. In recent years, Japanese researchers reported the correlation of rectal bleeding with the dose-volume parameter of rectum in patients with cervical cancer.[15,16] Isohashi *et al.* reported that the mean biologically equivalent dose in 2-Gy fraction (EQD2) of rectum D1cc for patients with and without rectal bleeding was 76 Gy and 98 Gy, respectively, and there was a significant greater rectal bleeding risk for the high EQD2 group (≥ 82 Gy of D1cc rectum).[15] In the current case, EQD2 of rectum D1cc was 79.9 Gy, which was calculated as the linear quadratic model for incomplete sublethal damage repair. If the dose prescription at point A could be increased by conventional ICBT until the dose of D90 for HRCTV reached 6 Gy, D1cc of the rectum would increase from 4.8 Gy to 8.2 Gy, and EQD2 of rectum D1cc would increase to 96.8 Gy. This method was able to increase the HRCTV dose while keeping the rectum dose at tolerable levels even in the case of bulky and/or irregular-shape cervical cancer. In the present case, primary tumor was well controlled without severe toxicities. However, further follow-up will be needed to confirm long-term efficacy and toxicities.

Historically, interstitial brachytherapy was performed with free hand-placement, and ultrasound-guided, CT-guided and template-guided needles for locally advanced tumor.[17–21] To date, transperineal template techniques were the most commonly used methods for interstitial treatment in such cases. However, these techniques have difficulties in achieving accurate positioning of the implant and good parallelism of the needles. In addition, using these methods, the applicators have to be left in place for a few days after implantation. On the other hand, a major part of the procedure in the current hybrid method is derived from conventional brachytherapy. In-room CT-guided insertion of the interstitial needle could be performed after implantation of the Fletcher-Suit applicator. Furthermore, because this insertion is done for each brachytherapy session, the applicators do not need to be left in place. Therefore, this hybrid method is a non-complicated technique and is safe for patients compared with previous methods.

Considering the risk of perforation of the sigmoid colon or intestine, accurate positioning of the needle in interstitial brachytherapy is very important. Several researchers have reported achieving accurate positioning and avoiding perforation by several methods.[17–21] With the present hybrid method, CT-guided insertion is performed after implantation of tandem and ovoid applicators. In addition, an in-room CT system is used for the current method. This system enabled implantation of the applicator, CT-guided placement of the needle and irradiation by RALS to be performed on the same couch. Movement of the applicator and needle can be min-

imized during implantation, planning and irradiation. Because of the CT-guided insertion and in-room system, accurate positioning and safe insertion can be achieved with this hybrid method.

Dimopuolos *et al.* and Kirisits *et al.* reported a similar technique of intracavitary and interstitial brachytherapy that uses a modified tandem-ring applicator for cervical cancer at Vienna University.[22,23] In their method, needles are inserted through holes in the tandem-ring applicator. As it is limited to moderate lateral expansion of the HRCTV, for cases with involvement up to the pelvic wall, additional interstitial needles are required. Their method was also accurate and safe, based on an MRI-guided approach. However, the Vienna ring applicator is not commercially available, and in Japan the most common type of applicator is the Fletcher-Suit Asian Pacific applicator. In our hybrid method, similar to the Vienna ring applicator, needles can be placed in the tumor located at the posterior parametrium with high flexibility. The current technique of brachytherapy should be further investigated to confirm its safety and efficacy.

REFERENCES

1. Nakano T, *et al* (2005) Long-term results of high-dose rate intracavitary brachytherapy for squamous cell carcinoma of the uterine cervix. Cancer **103**: 92–101.
2. Nakano T, *et al* (2010) Current advancement in radiation therapy for uterine cervical cancer. J Rad Res **51**: 1–8.
3. Rose PG and Bundy BN (2002) Chemoradiation for locally advanced cervical cancer: does it help? J Clin Oncol **20**: 891–893.
4. Eifel PJ, *et al* (2004) Pelvic irradiation with concurrent chemotherapy versus pelvic and para-aortic irradiation for high-risk cervical cancer: an update of radiation therapy oncology group trial (RTOG) 90-01. J Clin Oncol **22**: 872–880.
5. Pearcey R, *et al* (2002) Phase III trial comparing radical radiotherapy with and without cisplatin chemotherapy in patients with advanced squamous cell cancer of the cervix. J Clin Oncol **20**: 966–972.
6. Keys HM, *et al* (1999) Cisplatin, radiation, and adjuvant hysterectomy compared with radiation and adjuvant hysterectomy for bulky stage IB cervical carcinoma. N Engl J Med **340**: 1154–1161.
7. Goksedef BP, *et al* (2009) Concurrent cisplatin-based chemoradiation International Federation of Gynecology and Obstetrics stage IB2 cervical carcinoma. Am J Obstet Gynecol **200**: 175.e1–5.
8. Stehman FB, *et al* (2007) Radiation therapy with or without weekly cisplatin for bulky stage 1B cervical carcinoma: follow-up of a Gynecologic Oncology Group trial. Am J Obstet Gynecol **197**: 503.e1–6.
9. Whitney CW, *et al* (1999) Randomized comparison of fluorouracil plus cisplatin versus hydroxyurea as an adjunct to radiation therapy in stage IIB-IVA carcinoma of the cervix with negative para-aortic lymph nodes: a Gynecologic Oncology Group and Southwest Oncology Group study. J Clin Oncol **17**: 1339–1348.
10. Shepherd JH (1996) Cervical and vulva cancer: Changes in FIGO definitions of staging. Br J Obstet Gynaecol **103**: 405–406.
11. Owen R, *et al* (2010) A comparison of in-room computerized tomography options for detection of fiducial markers in prostate cancer radiotherapy. Int J Radiat Oncol Biol Phys **77**: 1248–1256.
12. Ma CM, *et al* (2006) In-room CT techniques for image-guided radiation therapy. Med Dosim **31**: 30–39.
13. Haie-Meder C, *et al* (2005) Recommendations from Gynaecological (GYN) GEC-ESTRO Working Group (I): concepts and terms in 3D image based 3D treatment planning in cervix cancer brachytherapy with emphasis on MRI assessment of GTV and CTV. Radiother Oncol **74**: 235–245.
14. Pötter R, *et al* (2006) Recommendations from gynaecological (GYN) GEC ESTRO working group (II): concepts and terms in 3D image-based treatment planning in cervix cancer brachytherapy-3D dose volume parameters and aspects of 3D image-based anatomy, radiation physics, radiobiology. Radiother Oncol **78**: 67–77.
15. Isohashi F, *et al* (2010) Rectal dose and source strength of the high-dose-rate iridium-192 both affect late rectal bleeding after intracavitary radiation therapy for uterine cervical carcinoma. Int J Radiat Oncol Biol Phys **77**: 758–764.
16. Kato S, *et al* (2010) CT-based 3D dose-volume parameter of the rectum and late rectal complication in patients with cervical cancer treated with high-dose-rate intracavitary brachytherapy. J Rad Res **51**: 215–221.
17. Syed AM, *et al* (2002) Long-term results of low-dose-rate interstitial-intracavitary brachytherapy in the treatment of carcinoma of the cervix. Int J Radiat Oncol Biol Phys **54**: 67–78.
18. Martinez A, *et al* (1985) Combination of external beam irradiation and multiple-site perineal applicator (MUPIT) for treatment of locally advanced or recurrent prostatic, anorectal, and gynaecologic malignancies. Int J Radiat Oncol Biol Phys **11**: 391–398.
19. Nag S, *et al* (1998) Interstitial brachytherapy in the management of primary carcinoma of the cervix and vagina. Gynecol Oncol **70**: 27–32.
20. Kuipers T, *et al* (2001) HDR brachytherapy applied to cervical carcinoma with moderate lateral expansion: modified principles of treatment. Radiother Oncol **58**: 25–30.
21. Erickson B and Gillin MT (1997) Interstitial implantation of gynaecologic malignancies. J Surg Oncol **66**: 285–295.
22. Kirisits C, *et al* (2006) The Vienna applicator for combined intracavitary and interstitial brachytherapy of cervical cancer: design, application, treatment planning, and dosimetric results. Int J Radiat Oncol Biol Phys **65**: 624–630.
23. Dimopoulos JC, *et al* (2006) The Vienna applicator for combined intracavitary and interstitial brachytherapy of cervical cancer: clinical feasibility and preliminary results. Int J Radiat Oncol Biol Phys **66**: 83–90.

Received on July 16, 2010
Revision received on October 13, 2010
Accepted on October 21, 2010
J-STAGE Advance Publication Date: ●● ●, 201●

J. Radiat. Res. Advance Publication. This article may be modified at the final publication.

J. Radiat. Res., 51, 715–721 (2010)

Regular Paper

The Benefit of Small Bowel and Pelvic Bone Sparing in Excluding Common Iliac Lymph Node Region from Conventional Radiation Fields in Patients with Uterine Cervical Cancer: A Dosimetric Study

Takahiro OIKE*, Tatsuya OHNO, Masaru WAKATSUKI, Shin-ei NODA, Jun-ichi SAITOH, Tatsuji MIZUKAMI, Yuya YOSHIMOTO, Noriyuki OKONOGI, Hiroyuki KATOH, Kei SHIBUYA, Yoshiyuki SUZUKI, Hitoshi ISHIKAWA, Takeshi EBARA, Takeo TAKAHASHI and Takashi NAKANO

Uterine cervical cancer/Radiotherapy/Small bowel/Pelvic insufficiency fracture/Common iliac lymph node region.

The purpose of this study was to compare dose reduction to the small bowel and sacral bone by two-field and four-field techniques when the common iliac lymph node region is excluded from the radiation field in external beam radiotherapy of uterine cervical cancer. Thirteen patients with cervical cancer were entered into the study. Conventional treatment plans based on bony landmarks were made with parallel-opposed two-field technique (C2F) and four-field box technique (C4F). Modified C2F (M2F) and C4F (M4F) plans of excluding the common iliac lymph node region from the conventional radiation fields were created in reference to the bifurcations of pelvic arteries in computed tomography images. For each patient, the dose volume histograms for the small bowel and sacral bone resulting from the C2F, C4F, M2F, and M4F plans were compared. The volumes were obtained at 10 levels of prescribed dose, at increments of 10%, from 5 Gy to 50 Gy. By sparing both small bowel and sacral bone, the M2F and M4F plans were significantly better than the C2F and C4F plans at any dose level ($p < 0.05$), respectively. In addition, the M4F plan was significantly better than the M2F plan in sparing both small bowel at 10–50% of the prescribed dose ($p < 0.05$) and sacral bone at 40–100% of the prescribed dose ($p < 0.05$). The present study suggests that modified treatment planning could be useful for selected patients for reducing small bowel complications and insufficiency fracture after radiotherapy.

INTRODUCTION

Radiotherapy has an essential role in the treatment of uterine cervical cancer. Early-stage disease is highly curable by radiotherapy alone. Concurrent chemoradiotherapy improves overall survival for locally advanced cervical cancer in comparison with radiotherapy alone.[1–6] Radiotherapy for cervical cancer consists of external beam irradiation to the primary tumor and corresponding region of lymphatic drainage, and brachytherapy for the primary tumor.[7] The external beam component is conventionally delivered by a two-field or four-field technique.

Small bowel complication is one of the most common side effects in gynecologic patients undergoing radiotherapy. It has been pointed out that high-dose irradiation to the small bowel of the pelvis correlates with severe intestinal complications.[8–12] Pelvic insufficiency fracture is also a major concern after radiotherapy to the pelvis. Although radiation-induced pelvic insufficiency fracture has been considered to be rare,[13] several recent reports revealed that it is more common than previously believed.[14–16] Thus, pelvic bone should be excluded from radiation fields as much as possible.

Efforts for dose reduction to organs at risk (OARs) should be encouraged to achieve lower incidence of late complications without sacrificing local control. In the treatment planning of the two-field and four-field techniques, definition of the superior border of the fields varies among radiotherapy facilities. A survey of the Gynecologic Cancer Intergroup showed that the upper border of the pelvic field for cervical

*Corresponding author: Phone: +81(27)220-8383,
Fax: +81(27)220-8397,
E-mail: t-oike@med.gunma-u.ac.jp
Department of Radiation Oncology, Gunma University Graduate School of Medicine, 3-39-22, Showa-machi, Maebashi, Gunma 371-8511, Japan.
doi:10.1269/jrr.10046

cancer was set at L4/L5 in 50% of the facilities, L5/S1 in 12%, and computed tomography (CT)-based planning in 24%.[17] However, the quantitative benefit of a small pelvic field for normal tissue sparing has not been well documented. Recently, treatment planning based on CT has become wide-spread, a method that enables us to define the clinical target volume (CTV) of the pelvic lymph node region more precisely by reference to pelvic vessels.

The purpose of this study was to compare the dose reduction to the small bowel and sacral bone by two-field or four-field technique when the common iliac lymph node region is excluded from the radiation field in external beam radiotherapy of uterine cervical cancer.

MATERIALS AND METHODS

Patient characteristics

Between January and October 2009, 13 consecutive patients with cervical cancer treated with radiotherapy at the Department of Radiation Oncology of Gunma University Graduate School of Medicine were selected for this dosimetric study. The median age of the patients was 63 years (range, 41–82 years). The International Federation of Gynecology and Obstetrics stage was IB in 2 patients, IIB in 7, IIIA or IIIB in 3, and IVA in 1 patient.

Imaging

Each patient underwent a planning CT scan (LightSpeed; GE Healthcare, Buckinghamshire, UK) in supine position with vaginal tampon contrast. CT images with 5-mm slice thickness were taken from the L3–L4 interspace to the perineum. Bladder content was not restricted at the time of CT data acquisition.

Delineation

Contouring was performed by a radiation oncologist. Another radiation oncologist specializing in gynecologic oncology reviewed all delineated regions of interest. All target volumes and OARs were contoured on the axial CT slices of all patients. CTV included the cervical tumor, the whole uterus, parametrium, uterine appendage, upper half of the vagina and regional lymph nodes (common nodes, internal and external iliac nodes, obturator nodes and presacral nodes). The small bowel of the pelvis and sacral bone were contoured as OARs. For the small bowel, individual loops existing below the level of the upper border of L5 vertebra were separately contoured. Common, internal and external iliac vessels were contoured as reference landmarks to identify the pelvic lymph node regions.

Treatment planning

All treatment plans and dose volume histogram (DVH) analysis were done with the treatment planning system XiO, Version 4.34 (CMS, St. Louis, MO, USA). All treatment plans were based on a 10-MV high-energy photon beam. For each patient, 4 treatment plans were generated as follows.

First, treatment plans based on a conventional parallel-opposed two-field technique (C2F) and four-field box technique (C4F) were made. The definition was based on the commonly used design of standard portals in relation to bony reference landmarks. The borders for the anterior and posterior fields were at the interspace of the L4–L5 vertebrae superiorly, inferior border of the obturator foramen inferiorly, and 1.5–2 cm lateral to the bony pelvis.

For the lateral field, the anterior border was placed 3 cm anterior to the vessel edge and posterior edge of the pubic symphysis. The posterior margin was defined 1.5 cm from the anterior aspect of the sacral bone. Superior and inferior borders were the same as those of the anterior and posterior fields. The width of the lateral fields was maintained at 6 cm at least to ensure coverage of the lymph node regions. The typical radiation fields of the conventional plans are shown in Fig. 1.

Second, modified plans of C2F and C4F were created. The common iliac lymph nodes are adjacent to the common iliac vessels from the aortic bifurcation to the division of the common iliac artery into the external and internal iliac branches.[18–21] In the modified C2F (M2F) and C4F (M4F) plans, the common iliac lymph node region was excluded from the conventional radiation fields. In case of different levels of bifurcation of the common iliac artery, the most cranial one was selected as the superior border. Inferior, lateral, anterior and posterior borders were defined just as those of C2F and C4F. The typical radiation fields of the modified plans are shown in Fig. 2.

For each plan, the total dose of 50 Gy in 25 fractions at the isocenter was prescribed. The beams were weighted equally in each portal in all plans. The planning target volume (PTV) had to be covered between 95% and 107% of the prescribed dose in the isocenter plane.

DVH analysis

For the small bowel of the pelvis and sacral bone, the percent volumes irradiated in the C2F, C4F, M2F, and M4F plans were compared. The volumes were obtained at 10 levels of prescribed dose, at increments of 10%, from 5 Gy to 50 Gy.

Statistical analysis

Statistical analysis was performed by StatMateIII Version 3.17 (ATMS, Tokyo, Japan). Paired t test was used to compare the different treatment plans. Differences were considered significant at $p < 0.05$.

RESULTS

Example case

The M4F plan for a representative patient is shown in Fig. 3. As seen in the sagittal image of Fig. 3, the volumes of the small bowel and the sacral bone were excluded from the lat-

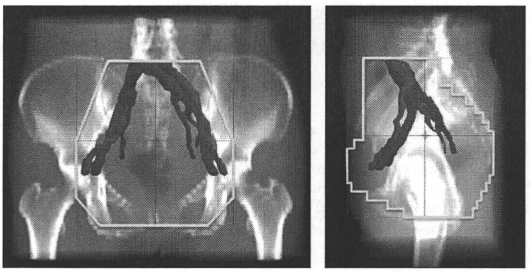

Fig. 1. Ventral and lateral radiation fields of conventional plan. Highlighted yellow lines are the border of the fields. Pelvic (common, internal and external) arteries and veins are illustrated in red and blue, respectively.

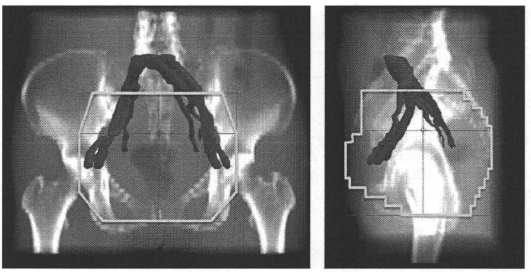

Fig. 2. Ventral and lateral radiation fields of modified plan. Highlighted yellow lines are the border of the fields. Common iliac lymph node region is excluded from the radiation fields. Pelvic (common, internal and external) arteries and veins are illustrated in red and blue, respectively.

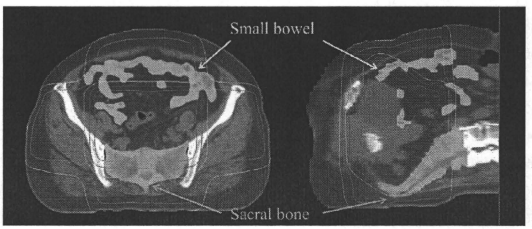

Fig. 3. Axial and sagittal images with isodose distribution in modified four-field plan. Highlighted are the 20% (orange), 50% (magenta), 70% (cyan), 90% (blue), and 100% (red) isodose lines. The small bowel and the sacral bone in these slices are shown in yellow and green, respectively.

eral radiation fields as much as possible. The average field size of 2.8 cm (range, 0.5–4.7 cm) was reduced in the longitudinal direction with the modified plans compared to the conventional plans.

Small bowel

Comparison of small bowel volumes irradiated in a representative patient is shown in Fig. 4. The volumes of the small bowel irradiated by each plan are summarized in Table 1. Compared to the C2F plan, the M2F plan was significantly better in sparing the small bowel at any dose level ($p < 0.001$). Through the total range of doses, the extent of volume reduction to the small bowel irradiated was similar. Compared to the C4F plan, the M4F plan was also significantly better in sparing the small bowel at any dose level ($p < 0.001$). A large extent of volume reduction was observed at 5–25 Gy. Compared to the M2F plan, the M4F plan was significantly better in sparing the small bowel at 5–25 Gy ($p < 0.001$ at 5–20 Gy, $p < 0.01$ at 25 Gy).

Sacral bone

Comparison of sacral bone volumes irradiated in a representative patient is shown in Fig. 5. The volumes of the sacral bone irradiated by each plan were summarized in Table 2.

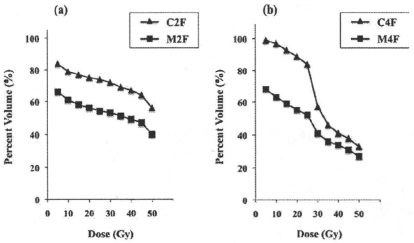

Fig. 4. Dose-volume-histogram for the small bowel. The percentages of small bowel volumes receiving different doses are shown. Comparison of conventional two-field (C2F) plan vs. modified two-field (M2F) plan is shown in (a), conventional four-field (C4F) plan vs.modified four-field (M4F) plan in (b).

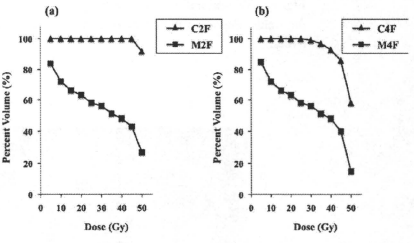

Fig. 5. Dose-volume-histogram for the sacral bone. The percentages of sacral bone volumes receiving different doses are shown. Comparison of conventional two-field (C2F) plan vs. modified two-field (M2F) plan is shown in (a), conventional four-field (C4F) plan vs. modified four-field (M4F) plan in (b).

Table 1. Median volumes of small bowel receiving prescribed doses with conventional and modified 2- or 4-field technique.

Dose	Median percent volume (range)			
	C2F	M2F	C4F	M4F
5	84 (76–100)	75 (47–87)	100 (99–101)	82 (52–100)
10	80 (70–100)	71 (41–84)	100 (97–101)	74 (45–100)
15	77 (67–100)	68 (37–83)	99 (89–100)	70 (40–99)
20	75 (65–98)	66 (35–81)	96 (81–98)	67 (37–97)
25	74 (63–96)	64 (33–80)	92 (72–98)	66 (34–95)
30	72 (59–88)	62 (31–79)	79 (52–92)	63 (30–90)
35	70 (55–79)	60 (29–78)	73 (38–83)	62 (27–83)
40	68 (50–77)	59 (27–77)	67 (29–77)	58 (23–80)
45	66 (43–75)	56 (24–75)	60 (20–78)	53 (17–78)
50	58 (22–69)	50 (16–69)	48 (9–75)	45 (8–75)

Abbreviations: C2F = conventional 2-field technique; M2F = modified 2-field technique; C4F = conventional 4-field technique; M4F = modified 4-field technique.

Table 2. Median volumes of sacral bone receiving prescribed doses with conventional and modified 2- or 4-field technique.

Dose	Median percent volume (range)			
	C2F	M2F	C4F	M4F
5	100 (100–100)	98 (84–100)	100 (100–100)	98 (85–100)
10	100 (100–100)	96 (81–100)	100 (100–100)	95 (72–100)
15	100 (100–100)	93 (76–100)	100 (100–100)	91 (66–100)
20	100 (100–100)	90 (74–100)	100 (100–100)	88 (63–100)
25	100 (100–100)	87 (70–100)	100 (100–100)	85 (56–100)
30	100 (98–100)	85 (68–100)	98 (87–100)	82 (56–98)
35	100 (94–100)	82 (51–100)	93 (75–100)	77 (51–98)
40	100 (89–100)	78 (48–100)	86 (66–99)	69 (48–96)
45	99 (81–100)	70 (43–100)	77 (53–98)	57 (40–92)
50	92 (42–99)	57 (27–96)	50 (24–88)	24 (12–72)

Abbreviations: C2F = conventional 2-field technique; M2F = modified 2-field technique; C4F = conventional 4-field technique; M4F = modified 4-field technique.

Compared to the C2F plan, the M2F plan was significantly better in sparing the sacral bone at any dose level ($p < 0.05$ at 5 Gy, $p < 0.01$ at 10–25 Gy, $p < 0.001$ at 30–50 Gy). Compared to the C4F plan, the M4F plan was significantly better in sparing the sacral bone at any dose level ($p < 0.05$ at 5–10 Gy, $p < 0.01$ at 15–25 Gy, $p < 0.001$ at 30–50 Gy). Compared to the M2F plan, the M4F plan was significantly better in sparing the sacral bone at 20–50 Gy of the prescribed dose ($p < 0.05$ at 20 Gy, $p < 0.01$ at 25 Gy, $p < 0.001$ at 30–50 Gy).

DISCUSSION

The Japanese Patterns of Care Study demonstrated the patterns of definitive radiotherapy practice for patients with uterine cervical cancer between 1999 and 2001 in Japan. Pelvic external beam RT was given using an opposing anteroposterior (AP-PA) technique in 87% of the patients. The upper border of the pelvic field was at the L4–L5 interspace in 77% of the patients.[22] CT simulation is widely used for radiotherapy treatment planning today. However, for uterine cervical cancer, the two-field technique based on bony landmarks is still the common treatment planning method in Japan. In the present study, we compared the dose reduction by two-field and four-field techniques when the common iliac lymph node region is excluded from the radiation field in patients with uterine cervical cancer. Our results suggest that, compared to conventional technique, the modified technique of excluding the common iliac lymph node region from the conventional field significantly reduces the irradiated volume of the small bowel and sacral bone.

The severity of acute intestinal complications has been considered to correlate with the irradiated volume of the small bowel.[8] It has also been pointed out that high-dose irradiation to the small bowel correlates with severe late intestinal complications.[8–12] Ohara *et al.* reported that, in the pelvis, a large amount of small bowel exists in the area ranging over 8 cm from the L4–L5 interspace and below that occupies the upper side in conventional fields.[11] Therefore, exclusion of the common iliac lymph node region from conventional fields could result in reduction of the irradiated volume of the small bowel. The results of our study show that the modified plans are significantly better than the conventional ones in sparing the small bowel volume irradiated at all dose levels in both two-field and four-field techniques (Fig. 4), thereby indicating that radiotherapy by the modified techniques could lead to a reduction in small bowel complications.

Radiation-induced pelvic insufficiency fracture has been regarded as a rare complication in patients with gynecologic cancer.[13] However, recent studies have reported the incidence of pelvic insufficiency fracture as 8.2–17.9% after pelvic irradiation, a higher frequency than previously believed.[14–16] The most common site of pelvic insufficiency fracture is the sacral bone including the sacroiliac joints. Kwon *et al.* reported that 85% of patients with pelvic insufficiency fracture after pelvic irradiation had sacral involvement in their retrospective evaluation of MRI images.[16] For this reason, we evaluated the DVHs of sacral bone in this study. The modified plans proved to be significantly better than the conventional plans in sparing sacral bone volume irradiated in both two-field and four-field techniques at all dose levels, and especially at a high-dose level (Fig. 5). Because high-dose irradiation (> 50.4 Gy) to the pelvic bone is regarded one of the risk factors of pelvic insufficiency fracture,[23] radiotherapy by the modified technique could reduce this incidence.

Which of M2F and M4F is better when both small bowel and sacral bone sparing are taken into account? As for small bowel sparing, M4F was significantly better only at a low to middle-dose level compared to M2F. Regarding sacral bone sparing, M4F showed significant benefit at a high-dose level compared to M2F. Thus, it could be concluded that the M4F technique is better for both small bowel and sacral bone sparing compared to M2F.

The upper border of the modified field depends on the position of the division of the common iliac artery into external and internal iliac branches. Greer *et al.* demonstrated the position of the common iliac bifurcation based on intraoperative retroperitoneal measurements from 100 patients.[24] They showed that the mean level of the bifurcation was 1.7 cm above the lumbosacral prominence on the right and 1.4 cm above on the left, that both common iliac bifurcations were cephalad to the level of the lumbosacral prominence in 87% of patients, and that the mean level of the aortic bifurcation was 6.7 cm above the lumbosacral prominence. In our study, as our standard upper border is at the L4–L5 interspace, field-size reduction in the modified plan varied from 0.5 cm to 4.7 cm (mean, 2.8 cm) in the longitudinal direction, which was relatively smaller than those in the study by Greer *et al.*

Patient selection is important in adopting radiotherapy with small bowel and sacral bone sparing technique while maintaining curability of the disease. Squamous cell carcinoma of the cervix, which constitutes approximately 80% of all cervical cancers, commonly metastasizes to lymph nodes anterogradely along vessels from paracervical lymph nodes to common iliac lymph nodes. Sakuragi *et al.* reviewed surgically treated cervical cancer cases, reporting the incidence of pelvic lymph node metastasis in stage Ib, stage IIa, and stage IIb as 12%–22%, 10%–27%, 34%–43% respectively.[25] They also reported a positive rate for metastasis to common iliac lymph node of 9.1% in 208 cases with stage Ib to stage IIb.[26] However, when focusing on early-stage squamous cell carcinoma of the cervix (Stage I/II, tumor size ≤ 4 cm), the frequency of metastasis to common iliac lymph nodes was a lower 1.5%.[27] In the early-stage cases, the modified technique of excluding the common iliac

lymph node region can be indicated. Further study will be needed to investigate the incidence of small bowel complications and insufficiency fracture, and failure patterns after radiotherapy with the modified technique.

Since most patients with early-stage disease will be cured, major efforts should be made to reduce long-term complications while maintaining post-radiotherapy efficacy. A small study of 33 cervical cancer patients treated after hysterectomy with intensity-modulated radiation therapy (IMRT) and concurrent chemotherapy showed decreased gastrointestinal and genitourinary side effects, with local control comparable to that in patients treated with four-field box radiotherapy.[28] Recently, Kidd *et al.* reported clinical outcomes of 452 cervical cancer patients treated with IMRT or non-IMRT.[29] In that report, IMRT significantly decreased toxicity while maintaining disease control. IMRT was used in 27% of the patients with gynecologic cancer in the United States in 2004[30] and the use of IMRT for gynecological malignancy is also of interest in Japan. Therefore, comparison of the current modified plan with IMRT by excluding the common iliac lymph node region from the target will be necessary.

In conclusion, we have demonstrated that the modified radiation technique of excluding the common iliac lymph node region from the conventional radiation field has significant benefits for sparing the small bowel and sacral bone in the treatment of cervical cancer compared with a conventional two-field or four-field technique. In clinical practice, the modified technique could be useful for patients with early-stage squamous cell carcinoma of the cervix and lead to a reduction in small bowel complications and insufficiency fracture after radiotherapy.

REFERENCES

1. National Cancer Institute (1999) Concurrent chemoradiation for cervical cancer. Clinical announcement.
2. Eifel PJ, *et al* (2004) Pelvic irradiation with concurrent chemotherapy versus pelvic and para-aortic irradiation for high-risk cervical cancer. J Clin Oncol **22**: 872–880.
3. Morris M, *et al* (1999) Pelvic radiation with concurrent chemotherapy compared with pelvic and para-aortic radiation for high-risk cervical cancer. N Engl J Med **340**: 1137–1143.
4. Rose PG, *et al* (1999) Concurrent cisplatin-based radiotherapy and chemotherapy for locally advanced cervical cancer. N Engl J Med **340**: 1144–1153.
5. Whitney CW, *et al* (1999) A randomized comparison of fluorouracil plus cisplatin versus hydroxyurea as an adjuvant to radiation therapy in stages IIB-IVA carcinoma of the cervix with negative para-aortic lymph nodes: A Gynecologic Oncology Group and Southwest Oncology Group study. J Clin Oncol **17**: 1339–1348.
6. Green JA, *et al* (2001) Survival and recurrence after concomitant chemotherapy and radiotherapy for cancer of the uterine cervix: a systematic review and meta-analysis. Lancet **358**: 781–786.
7. Nakano T, *et al* (2010) Current advancement in radiation therapy for uterine cervical cancer. J Radiat Res (Tokyo). **51**: 1–8.
8. Gallagher MJ, *et al* (1986) Prospective study of treatment technique to minimize the volume of pelvic small bowel with reduction of acute and late effects associated with pelvic irradiation. Int J Radiat Oncol Biol Phys **9**: 1565–1573.
9. Ferrigno R, *et al* (2001) High-dose-rate brachytherapy in the treatment of uterine cervix cancer. Analysis of dose effectiveness and late complications. Int J Radiat Oncol Biol Phys **50**: 1123–1135.
10. Letschert JG, *et al* (1990) Dose-volume correlation in radiation-related late small-bowel complications: a clinical study. Radiother Oncol **18**: 307–320.
11. Ohara K, *et al* (2004) Use of the small pelvic field instead of the classic whole pelvic field in postoperative radiotherapy for cervical cancer: reduction of adverse events. Int J Radiat Oncol Biol Phys **60**: 258–264.
12. Nakano T, *et al* (2005) Long-term results of high-dose rate intracavitary brachytherapy for squamous cell carcinoma of uterine cervix. Cancer **103**: 92–101.
13. Konski A and Sowers M (1996) Pelvic fractures following irradiation for endometrial carcinoma. Int J Radiat Oncol Biol Phys **35**: 361–367.
14. Ogino I, *et al* (2003) Pelvic insufficiency fractures in postmenopausal woman with advanced cervical cancer treated by radiotherapy. Radiother Oncol **68**: 61–67.
15. Ikushima H, *et al* (2006) Pelvic bone complications following radiation therapy of gynecologic malignancies: Clinical evaluation of radiation-induced pelvic insufficiency fractures. Gynecol Oncol **103**: 1100–1104.
16. Kwon JW, *et al* (2008) Pelvic bone complications after radiation therapy of uterine cervical cancer: evaluation of MRI. Am J Roentgenol **191**: 987–994.
17. Gaffney DK, *et al* (2007) Practice patterns of radiotherapy in cervical cancer among member groups of the Gynecologic Cancer Intergroup (GCIG). Int J Radiat Oncol Biol Phys **68**: 485–490.
18. Taylor A, *et al* (2005) Mapping pelvic lymph nodes: guidelines for delineation in intensity-modulated radiotherapy. Int J Radiat Oncol Biol Phys **63**: 1604–1612.
19. Taylor A, Rockall AG and Powell MEB (2007) An atlas of the pelvic lymph node regions to aid radiotherapy target volume definition. Clin Oncol **19**: 542–550.
20. Vilarino-Varela MJ, *et al* (2008) A verification study of proposed pelvic lymph node localization guidelines using nanoparticle-enhanced magnetic resonance imaging. Radiother Oncol **89**: 192–196.
21. Small W, *et al* (2008) Consensus guidelines for delineation of clinical target volume for intensity-modulated pelvic radiotherapy in postoperative treatment of endometrial and cervical cancer. Int J Radiat Oncol Biol Phys **71**: 428–434.
22. Toita T, *et al* (2008) Patterns of radiotherapy practice for patients with cervical cancer (1999–2001): Patterns of care study in Japan. Int J Radiat Oncol Biol Phys **70**: 788–794.
23. Oh D, *et al* (2008) Pelvic insufficiency fracture after radiotherapy for cervical cancer: Analysis of risk factors. Int J Radiat Oncol Biol Phys **70**: 1183–1188.
24. Greer BE, *et al* (1990) Gynecologic radiotherapy fields

defined by inraoperative measurements. Gynecol Oncol **38**: 421–424.
25. Sakuragi N (2007) Up-to-date management of lymph node metastasis and the role of tailored lymphadenectomy in cervical cancer. Int J Clin Oncol **12**: 165–175.
26. Sakuragi N, *et al* (1999) Incidence and distribution patterns of pelvic and paraaortic lymph node metastasis in patients with stage IB, IIA, and IIB cervical carcinoma treated with radical hysterectomy. Cancer **85**: 1547–1554.
27. Benedetti PP, *et al* (1996) Lymphatic spread of cervical cancer: an anatomical and pathological study based on 225 radical hysterectomies with systematic pelvic and aortic lymphadenectomy. Gynecol Oncol **62**: 19–24.
28. Chen MF, *et al* (2007) Clinical outcome in post hysterectomy cervical cancer patients treated with concurrent Cisplatin and intensity-modulated pelvic radiotherapy: Comparison with conventional radiotherapy. Int J Radiat Oncol Biol Phys **67**: 1438–1444.
29. Kidd EA, *et al* (2010) Clinical outcomes of definitive intensity-modulated radiation therapy with fluorodeoxyglucose-positron emission tomography simulation in patients with locally advanced cervical cancer. Int J Radiat Oncol Biol Phys **77**: 1085–1091.
30. Mell LK, Mehrotra AK and Mundt AJ (2005) Intensity-modulated radiation therapy use in the U.S., 2004. Cancer **104**: 1296–1303.

Received on April 11, 2010
Revision received on August 27, 2010
Accepted on August 31, 2010
J-STAGE Advance Publication Date: October 20, 2010

J. Radiat. Res., 51, 215–221 (2010)

Regular Paper

CT-based 3D Dose-Volume Parameter of the Rectum and Late Rectal Complication in Patients with Cervical Cancer Treated with High-Dose-Rate Intracavitary Brachytherapy

Shingo KATO[1]*, TRAN Dang Ngoc Linh[2], Tatsuya OHNO[3], Takashi NAKANO[4], Hiroki KIYOHARA[1], Yu OHKUBO[1] and Tadashi KAMADA[1]

Cervical cancer/High-dose-rate intracavitary brachytherapy/3D image-based brachytherapy/Late rectal complication/Dose-volume histogram.

This study evaluated the efficacy of computed tomography (CT)-based three-dimensional (3D) dose-volume parameters of the rectum as predictor for late rectal complication (LRC) in cervical cancer patients treated with radiotherapy alone. Eighty-four patients treated with a combination of external radiotherapy and high-dose-rate intracavitary brachytherapy between January 2000 and December 2004 were retrospectively analyzed. Brachytherapy was prescribed with standard 2D planning. Patients underwent pelvic CT at brachytherapy. The external rectal wall was contoured on the CT images, and the minimum doses delivered to 0.1cc, 1cc, and 2cc of the most irradiated rectal volumes were calculated with dose-volume histograms. The International Commission of Radiation Units and Measurements (ICRU) rectal point dose was also calculated by conventional method. Total dose (external radiotherapy plus brachytherapy) to the rectum was transformed to the biologically equivalent dose in 2-Gy fractions with α/β of 3 Gy ($D_{0.1cc}$, D_{1cc}, D_{2cc} and D_{ICRU}). The relationships between these dosimetric parameters and the incidence of LRC were analyzed. The 5-year overall actuarial rate of LRC was 26.4%. The values of $D_{0.1cc}$, D_{1cc}, and D_{2cc} were significantly higher in patients with LRC than in those without ($p < 0.001$), but the difference in the values of D_{ICRU} was not statistically significant ($p = 0.10$). The rate of LRC increased significantly with increasing $D_{0.1cc}$, D_{1cc}, and D_{2cc} ($p = 0.001$). However, no positive dose-response relationship was observed between D_{ICRU} and the rate of LRC ($p = 0.42$). The present study has suggested that CT-based 3D dose-volume parameters of the rectum may be effective for predicting LRC.

INTRODUCTION

Intracavitary brachytherapy (ICBT) is an important treatment modality for carcinoma of the urterine cervix. Because this treatment is characterized by a steep dose gradient, it can deliver a high dose to the cervical tumor while minimizing doses to the surrounding normal tissues. In some cases, however, the rectum, sigmoid colon, and/or bladder are irradiated with high doses because of close proximity to the cervical tumor, and this may result in late radiation complications.[1,2)]

Late rectal complication (LRC) is one of the most important dose-limiting toxicities, as severe LRC, such as a rectal ulcer or fistula, can be life-threatning. To assess the rectal dose of ICBT, X-ray-based two-dimensional (2D) treatment planning has tradionally been performed, and the International Commission on Radiation Units and Measurements (ICRU) rectal reference point has been used as the standard dose-specific point.[3)] Several investigators reported a positive correlation between the ICRU rectal point dose and the occurrence of LRC by the treatment of either low-dose-rate (LDR) or high-dose-rate (HDR) brachytherapy.[4–7)] However, several other investigators could not find a positive correlation between them.[8–10)] Because the ICRU rectal point is a

*Corresponding author: Phone: +81-43-206-3360,
Fax: +81-43-256-6506,
E-mail: s_kato@nirs.go.jp

[1]Research Center Hospital for Charged Particle Therapy, National Institute of Radiological Sciences, 4-9-1, Anagawa, Inage-ku, Chiba, 263-8555, Japan; [2]Department of Gynecology, Ho Chi Minh City Cancer Hospital, 03 No Trang Long Street, Binh Thanh District, Ho Chi Minh City, Viet Nam; [3]Gunma University Heavy Ion Medical Center; [4]Department of Radiology and Radiation Oncology, Gunma University Graduate School of Medicine, 3-39-22, Showa-machi, Maebashi, Gunma, 371-8511, Japan.

Presented in part at the 2008 World Congress of Brachytherapy, May 4-6, 2008, Boston, MA.

Conflicts of Interest Statement: The authors indicate no potential conflicts of interest.

doi:10.1269/jrr.09118

hypothetical point determined by the two orthogonal X-rays, it may not always represent the exact location of the highest dose in the rectum.[11,12]

Recently, computed tomography (CT) and magnetic resonance imaging (MRI) have increasingly been used for treatment planning of ICBT for cervical cancer, as these imaging modalities provide more accurate information than orthogonal X-rays on the topographic relationship between applicators, the cervical tumor and organs at risk (OARs). Treatment planning using CT or MRI images also allows assessment of three-dimensional (3D) dose distributions and dose-volume evaluation for tumor and OARs. The Group Européen de Curiethérapie-European Society for Therapeutic Radiology and Oncology (GEC-ESTRO) working group for gynecologic brachytherapy has provided recommendations on 3D image-based treatment planning in cervical cancer brachytherapy.[13,14] To assess the rectal dose by ICBT, 3D dose-volume parameters, including the minimum doses delivered to 0.1cc, 1cc, and 2cc of the most irradiated rectal volume, are recommended for recording and reporting. Several authors have reported that 3D image-based brachytherapy, according to the GEC-ESTRO recommendations, could improve target volume coverage and reduce doses to OARs.[15,16] However, only a few reports have been published on the relationship between the 3D dose-volume parameters and clinical outcomes.[17–20] Especially, dose-response relationships between the 3D dose-volume parameters of the rectum and LRC have not been thoroughly evaluated clinically.

Since a CT scanner was installed in the ICBT treatment room of our hospital in 2000, we have been taking pelvic CT images at ICBT with the applicators in place. After treatment, almost all patients underwent long-term follow-up, and clinical data on disease status, early and late radiation complications, quality of life, and life and death were recorded. We have already reported a positive correlation between the maximum rectal dose calculated by CT images and the incidence of LRC.[21] In the present study, we analyzed the relationship between CT-based 3D dose-volume parameters of the rectum and the incidence of LRC. The objective of this study was to evaluate the efficacy of the dose-volume parameters as predictor for LRC in cervical cancer patients treated with definitive radiotherapy.

METHODS AND MATERIALS

Patients

Eighty-four patients treated with radiotherapy alone between January 2000 and December 2004 were retrospectively analyzed. As the pure radiation dose-volume effect to the rectum was investigated in the present study, patients treated with chemoradiotherapy were excluded. All patients (median age 69 years, range 30–86) had previously untreated cervical cancer, and according to the International Federation of Gynecology and Obstetrics (FIGO) staging system, 19 patients had Stage IB, 37 had Stage II, 20 had Stage III, and 8 had Stage IVA disease. Histologically, 79 patients had squamous cell carcinoma and 5 had adenocarcinoma or adenosquamous carcinoma. All patients underwent CT of the abdomen and pelvis and MRI of the pelvis before treatment. Cervical tumor dimensions were measured based on T2-weighted MRI images. Forty-six patients had tumors < 4 cm and 38 had tumors ≥ 4 cm in maximum diameter.

Radiotherapy

Patients were treated with a combination of external beam radiotherapy (EBRT) and HDR-ICBT according to the Japanese treatment guidelines.[22] EBRT was delivered to the whole pelvis through anterior and posterior parallel-opposed portals using 10-MV X-rays with a daily fraction dose of 1.8 or 2.0 Gy. The median total dose delivered to the pelvic sidewall was 50 Gy (range, 36–60.6 Gy). In principle, a central shield (3–4 cm width at the isocenter) was inserted into the treatment field after delivering 19.8 Gy to the whole pelvis in patients with early-stage disease (stage I–II and tumor size ≤ 4 cm in maximum diameter). In patients with advanced-stage disease (stage III–IVA or tumor size > 4 cm in maximum diameter), a central shield was usually inserted after 30.6 Gy of whole pelvic irradiation.

HDR-ICBT was performed using the ^{192}Ir remote afterloading system (microSelectron, Nucletron, Veenendaal, The Netherlands). A combination of tandem and ovoid applicators was used for most patients. A combination of tandem and vaginal cylinder was used for some patients with narrow vagina or those with tumor infiltration to the lower vagina. A foley catheter was inserted and ballooned with 7 ml of contrast medium to localize the bladder neck. The bladder was filled with 100 ml of normal saline to avoid high-dose irradiation to the whole volume of the bladder. Bowel preparation was performed to achieve an empty rectum and sigma. After implantation of the applicators, two orthogonal X-rays were taken, and standard 2D treatment planning was performed using the treatment planning system (Plato BPS, version 13.7, Nucletron, Veenendaal, The Netherlands). HDR-ICBT was performed once a week, concurrently with central-shielding EBRT. The median total point A dose of ICBT was 24 Gy in 4 fractions (range, 10–30 Gy).

3D dosimetry

Both a C-arm type X-ray unit and a CT scanner were installed in the treatment room. All patients underwent plain pelvic CT at brachytherapy with the applicators in place. After taking orthogonal radiographs, CT images with 5-mm slice thickness were taken in the same supine position on the same treatment couch. All CT images were electrically stored.

The contour of the rectum was determined by two radiation oncologists (S. K. and T. L.). According to the GEC-ESTRO recommendations,[13] the external rectal wall was delineated on the CT images using Oncentra Masterplan

(Nucletron). The contour of the rectum began at the anorectal junction and ended at the rectosigmoid flexure. For precise contour delineation, MRI and CT images at diagnosis were always referred to.

The CT data sets were imported into the treatment planning system (Plato BPS). The dose distribution generated by X-ray-based 2D planning was superimposed on the CT data set by matching the applicator positions (Fig. 1). A cumulative dose-volume histogram (DVH) of the rectum was calculated, and the minimum doses delivered to 0.1cc, 1cc, and 2cc of the most irradiated rectal volume were derived from the DVH according to the GEC-ESTRO recommendation.[14]

Many patients could undergo CT scans at the first session of ICBT only. Therefore, the cumulative dose to the rectum for all ICBT fractions was calculated by multiplying the corresponding dose by the fraction number of ICBT as the most practical method. Regarding the rectal dose from EBRT, it was assumed that the whole rectum received 100% of the prescribed EBRT dose before central shield.

When applying 3D dose volume assessments, the doses to the rectum from both EBRT and ICBT were normalized to the biologically equivalent doses in 2 Gy fractions (Gy_{EQD2}) based on the linear-quadratic model using an α/β ratio of 3 Gy. 3D dose-volume parameters of the rectum ($D_{0.1cc}$, D_{1cc}, and D_{2cc}) were calculated by adding the biologically equivalent doses of whole pelvic EBRT and all ICBT fractions. The dose at the ICRU rectal point was calculated in each ICBT session by conventional method, and the total dose at the ICRU rectal point was calculated with the same way (D_{ICRU}).

Assessment of late rectal complications

After treatment, patients were followed up monthly in the first year, bi-monthly in the second year, and every 3–4 months in the third to fifth years. Follow-up evaluation consisted of history-taking, physical examination, and routine blood tests. CT of the abdomen and pelvis and/or MRI of the pelvis were performed once or twice a year for most patients. Stool examination was indicated when LRC was suspected. Late rectal complications were graded according to the Radiation Therapy Oncology Group (RTOG)/European Organization of Research and Treatment of Cancer (EORTC) late radiation morbidity scoring scheme.[23]

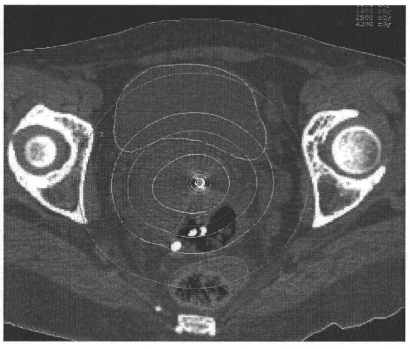

Fig. 1. Dose distributions of intracavitary brachytherapy projected onto the axial CT image.

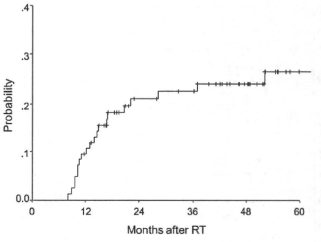

Fig. 2. Overall actuarial rate of late rectal complications.

Table 1. Comparison of the values of dosimetric parameters between patients with and without late rectal complications (all Grades).

parameter	LRC (–) n = 64 average (range) (Gy_{EQD2})	LRC (+) n = 20 average (range) (Gy_{EQD2})	p value
D_{ICRU}	73.9 (11.5–125.8)	83.4 (43.5–127.8)	p = 0.10
$D_{0.1cc}$	77.3 (15.0–157.2)	111.4 (54.8–156.1)	p < 0.001
D_{1cc}	61.7 (13.2–115.8)	85.4 (51.0–136.9)	p < 0.001
D_{2cc}	53.9 (12.1– 93.0)	72.0 (44.1– 99.3)	p < 0.001

Abbreviations: LRC, late rectal complication; EQD2, biologically equivalent dose in 2-Gy fractions; ICRU, International Commission on Radiation Units and Measurements.

Table 2. Comparison of the values of dosimetric parameters between patients with and without Grade 2 late rectal complications.

parameter	LRC (–) n = 77 average (range) (Gy_{EQD2})	LRC (+) n = 7 average (range) (Gy_{EQD2})	p value
D_{ICRU}	74.8 (11.5–125.8)	90.9 (46.7–127.8)	p = 0.07
$D_{0.1cc}$	83.8 (15.0–157.2)	104.1 (71.3–152.6)	P = 0.12
D_{1cc}	66.2 (13.2–136.9)	80.1 (65.8–119.5)	P = 0.12
D_{2cc}	57.2 (12.1– 99.3)	69.3 (56.2– 95.3)	P = 0.08

Abbreviations: LRC, late rectal complication; EQD2, biologically equivalent dose in 2-Gy fractions; ICRU, International Commission on Radiation Units and Measurements.

Statistical analysis

The two-sided paired t test was used to compare the distribution of the dosimetric parameters between patients with and without LRC. The overall actuarial rate of LRC was calculated using the Kaplan-Meier method. The time to LRC was measured from the date of radiotherapy initiation to the date of the first episode of LRC. Patients who died without complications were censored at the time of death, and surviving patients without complications were also censored at the date of their last follow-up. To analyze the dose-response relationship, patients were classified into several groups according to their values of dosimetric parameters, and the 5-year LRC rates for the respective groups were compared. The log-rank test was used for comparison. A p value ≤ 0.05 was considered to indicate a statistically significant difference.

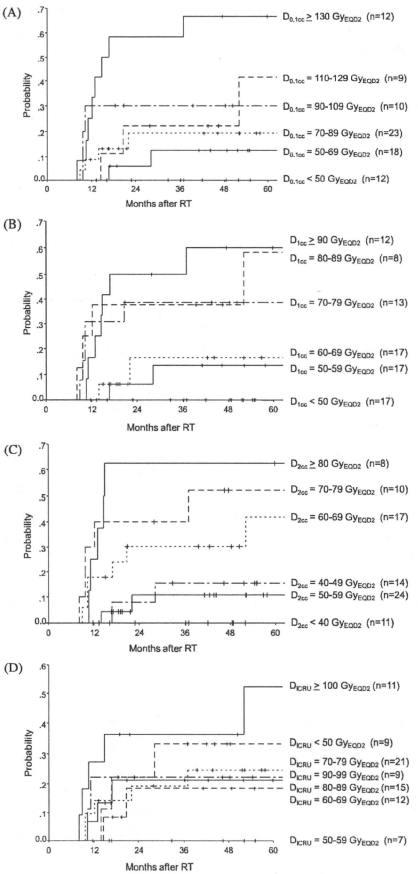

Fig. 3. Actuarial rates of late rectal complications by the values of $D_{0.1cc}$ (A), D_{1cc} (B), D_{2cc} (C), and D_{ICRU} (D) of the rectum. Abbreviations: EQD2, biologically equivalent dose in 2-Gy fractions

RESULTS

The median follow-up duration for all patients was 43.9 months (12 to 91 months). The 5-year overall survival and local control rates for all patients were 77.7% and 90.4%, respectively. Twenty (23.8%) patients developed LRC, 13 with Grade 1 and 7 with Grade 2. No severe (Grades 3–5) complication was observed. The 5-year actuarial rate of LRC was 26.4% (Fig. 2).

The values of $D_{0.1cc}$, D_{1cc}, D_{2cc}, and D_{ICRU} for patients with and without LRC are summarized in Table 1. The values of $D_{0.1cc}$, D_{1cc}, and D_{2cc} were significantly higher in patients with LRC than in those without ($p < 0.001$). Although the values of D_{ICRU} tended to be higher in patients with than without LRC, the difference between the two groups was not significant ($p = 0.10$). When the values of these dosimetric parameters were compared between patients with and without Grade 2 LRC, no statistically significant difference was observed (Table 2).

For dose-response relationship analysis, patients were classified into six groups with their values of dosimetric parameters by 10-Gy_{EQD2} (D_{1cc}, D_{2cc}, and D_{ICRU}) or 20-Gy_{EQD2} ($D_{0.1cc}$) increments. The actuarial rates of LRC for patients in the respective groups are shown in Fig. 3A–D. The LRC rate significantly increased with increasing $D_{0.1cc}$ ($p = 0.001$), D_{1cc} ($p = 0.001$), and D_{2cc} ($p = 0.001$). However, no positive dose-response relationship was observed between D_{ICRU} and the rate of LRC ($p = 0.42$).

DISCUSSION

In the treatment planning for cervical cancer brachytherapy, MRI- or CT-based 3D treatment planning is being increasingly used these days. To assess the dose to the rectum, 3D dose-volume parameters, including $D_{0.1cc}$, D_{1cc}, and D_{2cc} of the rectum calculated with DVH, are recommended for recording and reporting.[13,14] Several investigators reported the relationship between these 3D dose-volume parameters and clinical outcomes. Georg *et al.* calculated MRI-based dose-volume parameters and analyzed their correlation with clinical symptoms and rectosigmoidoscopic findings. They reported that D_{2cc} was significantly higher in patients with

clinical symptoms or moderate to severe mucosal changes than in those without.[18] Koom *et al.* compared CT-based dose-volume parameters with the findings of rectosigmoidoscopy, reporting that $D_{0.1cc-2cc}$ were significantly greater in patients with moderate to severe mucosal changes.[19] These data suggested that 3D dose-volume parameters may possess good predictive value for LRC. However, long-term follow-up data on dose-volume parameters are quite limited, and therefore the predictive value for LRC has still to be established.

In the present study, we calculated $D_{0.1cc}$, D_{1cc}, and D_{2cc} of the rectum using CT images according to the GEC-ESTRO recommendations and compared them with the incidence of LRC. To the best of our knowledge, this is the first study to analyze the relationship between 3D dose-volume parameters and the long-term incidence of LRC. Consequently, positive dose-response relationships were observed between $D_{0.1cc}$, D_{1cc}, and D_{2cc} and the incidence of LRC (Table 1, Fig. 3A–C). From the results, it was suggested that CT-based 3D dose-volume parameters of the rectum might be effective indicators for predicting LRC.

In the present study, however, no positive dose-response relationship was observed between $D_{0.1cc}$, D_{1cc}, and D_{2cc} and Grade 2 LRC, probably because of the small number of patients developing Grade 2 LRC (Table 2). Furthermore, it was not possible to examine the relationship between dose-volume parameters and severe LRC, as Grade 3–5 LRC was not seen in the study. Regarding the relationship between 3D dose-volume parameters and severe LRC, there have only been a few reports in the literature. Pötter *et al.* treated cervical cancer patients with MRI-based HDR-ICBT and reported a low rate of LRC (Grade 1–2, 4%; Grade 3–4, 0%). D_{2cc} of the rectum was limited to 75–78 Gy_{EQD2} in their series, and they suggested that the dose constraint had contributed to the low rate of LRC.[20] However, this dose constraint was based on clinical data from the relationship between the ICRU rectal point dose and moderate or severe LRC.[4–7] Therefore, further study is needed to evaluate the dose-response relationship between 3D dose-volume parameters and severe LRC and to determine the threshold dose for severe LRC.

Regarding the relationship between the ICRU rectal point dose and the incidence of LRC, several reports have demonstrated either positive or negative correlation between them.[4–10] In the present study, no significantly positive relationship was observed between D_{ICRU} and the incidence of LRC, although the values of D_{ICRU} tended to be higher in patients with than without LRC (Table 1, Fig. 3D). The dose distributions projected onto CT images demonstrated that, in some patients, the ICRU rectal point was not the exact location in the rectum receiving the highest dose. In these cases, the rectum was found to have shifted laterally, or the dose distributions were not symmetrical because of non-ideal applicator geometry. Several studies demonstrated either positive or negative correlation between 3D dose-volume parameters and the ICRU rectal dose, and this discrepancy might be explained by geometrical variations between applicators and rectum.[11,12,24–26] From these results, it was suggested that the ICRU rectal point dose might not always be a good predictor for LRC.

To calculate the rectal dose from EBRT, it was assumed that the whole rectum received 100% of the prescribed EBRT dose before central shield in the present study. However, inhomogeneity exists in EBRT dose distribution, even when anterior and posterior parallel-opposed portals or four-field box technique is used. Generally speaking, this dose inhomogeneity is not larger than ± 5% for the dose of EBRT, which is much smaller compared with that of ICBT. Therefore, according to the GEC-ESTRO recommendation, it should be assumed that a homogeneous dose is delivered to the rectum at EBRT.[14]

It was also assumed in the present study that the rectum was completely shielded from EBRT after inserting the midline block. However, the rectum meight be irradiated with some doses after central shield by the topographic relationship between the midline block and the rectum. But the rectal wall receiving a high dose at ICBT is always adjacent to the applicator. And it can be shielded from EBRT by the midline block unless the applicator position is shifted extremely laterally. Threfore, the possibility of receiving some EBRT doses after central shield is not considered to be of great concern in calculating $D_{0.1cc-2cc}$ of the rectum.

In assessing the doses to OARs, the GEC-ESTRO working group also recommends D_{5cc} and D_{10cc}, if contouring organ walls is performed.[14] Strictly speaking, the doses to the organ walls should be calculated in the assessment of late complications. However, it is generally difficult to manually delineate very small organ walls, especially the walls of the rectum and sigmoid colon. It is also difficult to have automatically generated second contours at selected distances by the current treatment planning system. When volumes smaller than 5cc are considered, the DVHs based on organ contour and organ wall contour can lead to almost identical numerical results.[12] Therefore, it is considered the practical way to calculate $D_{0.1cc-2cc}$ of the rectum from organ contouring only.

Although MRI is superior to CT in visualizing cervical tumors,[13,27] we used CT rather than MRI images because, as in many other institutions, the MRI unit is located far from the brachytherapy room. As for brachytherapy applicators, we have never used MRI-compatible non-metallic applicators, but we have used thin metallic tandem and ovoid applicators without tungsten shields. These applicators are less expensive than the MRI-compatible ones and can produce acceptable CT images with minimum image artifacts for contouring target volumes and OARs. Several investigators have described that the outer walls of the bladder and rectum were clearly visualized on CT images, although they had

some limitations in visualizing the cervical tumor and its extention.[13,28] Also in the present study, the external rectal walls were clearly visualized on CT images in most cases. Therefore, CT images are considered to be adequate for the DVH analysis of the rectum.

CT images at brachytherapy were generated with 5-mm slice thickness in the present study. However, when using this slice thickness, two problems arose in the 3D treatment planning of ICBT. One was positional inaccuracy in reconstructing the applicator geometry, and the other was volumetric inaccuracy in contouring the intricately shaped organs. Because the active dwell positions may be shifted, added, or skipped by at least 2.5-mm steps to optimize dose distribution,[15] we have now changed the imaging protocol and take CT images at 2.5-mm slice thickness.

In the present study, it was not feasible to perform CT scan at every ICBT session for several practical and logistical reasons. In fractionated ICBT, however, the doses to the bladder and rectum may change between fractions according to geometrical variations in the applicators and these organs. For accurate evaluation, it is preferable to perform 3D image-based treatment planning at every ICBT session.[29,30] Therefore, there was a limitation to the accuracy of the dose-volume parameters in the present study. Despite this limitation, the 3D dose-volume parameters analyzed here showed positive correlations with the incidence of LRC, giving impetus to further study. We are now making every effort to perform CT-based treatment planning at every ICBT session.

In conclusion, CT-based 3D dose-volume parameters of the rectum according to the GEC-ESTRO recommendations may represent effective predictors for LRC. Further study is needed to evaluate the dose-response relationship between 3D dose-volume parameters and severe LRC and to determine the threshold dose for severe LRC.

ACKNOWLEGEMENT

This study was supported by the Research Project with Heavy Ions at the National Institute of Radiological Sciences.

REFERENCES

1. Eifel PJ, *et al* (1995) Time course and incidence of late complications in patients treated with radiotherapy for FIGO stage IB carcinoma of the uterine cervix. Int J Radiat Oncol Biol Phys **32**: 1289–1300.
2. Nakano T, *et al* (2005) Long-term results of high-dose rate intracavitary brachytherapy for squamous cell carcinoma of the uterine cervix. Cancer **103**: 92–101.
3. International Commission on Radiation Units and Measurements (1985) ICRU report 38: Dose and volume specification for reporting intracavitary therapy in gynecology. Bethesda, MD: International Commission on Radiation Units and Measurements.
4. Perez CA, *et al* (1984) Radiation therapy alone in treatment of carcinoma of the uterine cervix: II. Analysis of complications. Cancer **54**: 235–246.
5. Pourquier H, Dubois JB and Deland R (1982) Cancer of the uterine cervix: dosimetric guidelines for prevention of late rectal and rectosigmoid complications as a result of radiotherapeutic treatment. Int J Radiat Oncol Biol Phys **8**: 1887–1895.
6. Clark BG, *et al* (1997) The prediction of late rectal complications in patients treated with high dose-rate brachytherapy for carcinoma of the cervix. Int J Radiat Oncol Biol Phys **38**: 989–993.
7. Kim TH, *et al* (2005) Dosimetric parameters that predict late rectal complications after curative radiotherapy in patients with uterine cervical carcinoma. Cancer **104**: 1304–1311.
8. Ferrigno R, *et al* (2001) High-dose-rate brachytherapy in the treatment of uterine cervix cancer. Analysis of dose effectiveness and late complications. Int J Radiat Oncol Biol Phys **50**: 1123–1135.
9. Kapp KS, *et al* (1997) Carcinoma of the cervix: analysis of complications after primary external beam radiation and Ir-192 HDR brachytherapy. Radiother Oncol **42**: 143–153.
10. Katz A and Eifel PJ (2000) Quantification of intracavitary brachytherapy parameters and correlation with outcome in patients with carcinoma of the cervix. Int J Radiat Oncol Biol Phys **48**: 1417–1425.
11. Van den Berg F, *et al* (1998) The use of transverse CT image for the estimation of the dose given to the rectum in intracavitary brachytherapy for carcinoma of the cervix. Radiother Oncol **47**: 85–90.
12. Wachter-Gerstner N, *et al* (2003) Bladder and rectum dose defined from MRI based treatment planning for cervix cancer brachytherapy: Comparison of dose-volume histograms for organ contours and organ wall, comparison with ICRU rectum and bladder reference point. Radiother Oncol **68**: 269–276.
13. Haie-Meder C, *et al* (2005) Recommendations from Gynaecological (GYN) GEC-ESTRO Working Group (I): Concepts and terms in 3D image based 3D treatment planning in cervix cancer brachytherapy with emphasis on MRI assessment of GTV and CTV. Radiother Oncol **74**: 235–245.
14. Pötter R, *et al* (2006) Recommendations from gynaecological (GYN) GEC ESTRO working group (II): Concepts and terms in 3D image-based treatment planning in cervix cancer brachytherapy - 3D dose volume parameters and aspects of 3D image-based anatomy, radiation physics, radiobiology. Radiother Oncol **78**: 67–77.
15. Kirisits C, *et al* (2005) Dose and volume parameters for MRI-based treatment planning in intracavitary brachytherapy for cervical cancer. Int J Radiat Oncol Biol Phys **62**: 901–911.
16. Lang S, *et al* (2006) Intercomparison of treatment concepts for MR image assisted brachytherapy of cervical carcinoma based on GEC-ESTRO recommendations. Radiother Oncol **78**: 185–193.
17. Dimopoulos J, *et al* (2009) Dose-volume histogram parameters and local tumor control in magnetic resonance image-guided cervical cancer brachytherapy. Int J Radiat Oncol Biol Phys **75**: 56–63.
18. Georg P, *et al* (2009) Correlation of dose-volume parameters,

endoscopic and clinical rectal side effects in cervix cancer patients treated with definitive radiotherapy including MRI-based brachytherapy. Radiother Oncol **91**: 173–180.

19. Koom WS, *et al* (2007) Computed tomography-based high-dose-rate intracavitary brachytherapy for uterine cervical cancer: Preliminary demonstration of correlation between dose-volume parameters and rectal mucosal changes observed by flexible sigmoidoscopy. Int J Radiat Oncol Biol Phys **68**: 1446–1454.
20. Pötter R, *et al* (2006) 3D conformal HDR-brachy- and external beam therapy plus simultaneous Cisplatin for high-risk cervical cancer: Clinical experience with 3 year follow-up. Radiother Oncol **79**: 80–86.
21. Noda S, *et al* (2007) Late rectal complications evaluated by computed tomography-based dose calculations in patients with cervical carcinoma undergoing high-dose-rate brachytherapy. Int J Radiat Oncol Biol Phys **69**: 118–124.
22. Japan Society of Obstetrics and Gynecology, The Japanese Pathological Society, and Japan Radiological Society, editors (1987) The general rules for clinical and pathological management of uterine cervical cancer. Kanehara Shuppan, Tokyo.
23. Cox JD, Stetz J and Pajak TF (1995) Toxicity criteria of the Radiotherapy Oncology Group (RTOG) and the European Organization for Research and Treatment of Cancer (EORTC). Int J Radiat Oncol Biol Phys **31**: 1341–1346.
24. Pelloski CE, *et al* (2005) Comparison between CT-based volumetric calculations and ICRU reference-point estimates of radiation doses delivered to bladder and rectum during intracavitary radiotherapy for cervical cancer. Int J Radiat Oncol Biol Phys **62**: 131–137.
25. Yaparpalvi R, *et al* (2008) Point vs. Volumetric bladder and rectal doses in combined intracavitary-interstitial high-dose-rate brachytherapy: Correlation and comparison with published Vienna applicator data. Brachytherapy **7**: 336–342.
26. Wang B, *et al* (2009) Image-guided intracavitary high-dose-rate brachytherapy for cervix cancer: A single institutional experience with three-dimensional CT-based planning. Brachytherapy **8**: 240–247.
27. Nag S, *et al* (2004) Proposed guidelines for image-based intracavitary brachytherapy for cervical carcinoma: Report from image-guided brachytherapy working group. Int J Radiat Oncol Biol Phys **60**: 1160–1172.
28. Viswanathan AN, *et al* (2007) Computed tomography versus magnetic resonance imaging-based contouring in cervical cancer brachytherapy: Results of a prospective trial and preliminary guidelines for standardized contours. Int J Radiat Oncol Biol Phys **68**: 491–498.
29. Hellebust TP, *et al* (2001) Inter fraction variations in rectum and bladder volumes and dose distributions during high dose rate brachytherapy treatment of the uterine cervix investigated by repetitive CT-examinations. Radiother Oncol **60**: 273–280.
30. Kirisits C, *et al* (2006) Uncertainties when using only one MRI-based treatment plan for subsequent high-dose-rate tandem and ring applicators in brachytherapy for cervix cancer. Radiother Oncol **81**: 269–275.

Received on October 1, 2009
Revision received on November 11, 2009
Accepted on November 25, 2009

J. Radiat. Res., 51, 707–713 (2010)

Regular Paper

Depth Scaling of Solid Phantom for Intensity Modulated Radiotherapy Beams

Yukio FUJITA[1]*, Naoki TOHYAMA[2], Atsushi MYOJOYAMA[1] and Hidetoshi SAITOH[1]

Solid phantom/Depth scaling/Beam hardening effect/Multileaf collimator/Intensity modulated radiotherapy.

To reduce the uncertainty of absorbed dose for high energy photon beams, water has been chosen as a reference material by the dosimetry protocols. However, solid phantoms are used as media for absolute dose verification of intensity modulated radiotherapy (IMRT). For the absorbed dose measurement, the fluence scaling factor is used for converting an ionization chamber reading in a solid phantom to absorbed dose to water. Furthermore the depth scaling factor is indispensable in determining the fluence scaling factor. For IMRT beams, a photon energy spectrum is varied by transmitting through a multileaf collimator and attenuating in media. However, the effects of spectral variations on depth scaling have not been clarified yet. In this study, variations of photon energy spectra were determined using the EGS Monte Carlo simulation. The depth scaling factors for commercially available solid phantoms were determined from effective mass attenuation coefficients using photon energy spectra. The results clarified the effect of spectral variation on the depth scaling and produced an accurate scaling method for IMRT beams.

INTRODUCTION

For the recent national and international dosimetry protocols, water has been chosen as a reference material. However, dose measurement in water is sometimes impractical, so a solid phantom is used as a substitute for water. An example is dosimetric quality assurance of intensity modulated radiotherapy (IMRT) because a solid phantom is easier to set up than water and it can reproduce complex geometry such as anthropomorphic phantoms.

For photon beams, Seuntjens *et al.* reported a method to determine absorbed dose to water by ionization chamber measurement in solid phantoms.[1)] In their report, the "phantom dose conversion factor" is used to convert an ionization chamber reading in a solid phantom to absorbed dose to water. The factor is also known as the fluence scaling factor in the IAEA TRS-398.[2)] The factor can be determined experimentally as a ratio of ionization chamber reading in water at a reference depth to reading in a solid phantom at an equivalent depth. The equivalent depth was determined by applying the scaling theorem.[2,3)] In their report, depth can be scaled using a constant ratio of electron densities of two media. The scaling theorem assumes that photons interact with a medium only by the Compton scatter even if the pair-production accounts for 20% of total interaction for 10 MeV photon in water. Therefore, all phenomena of interactions with a medium should be considered for the depth scaling for megavoltage photon beams.

For IMRT beams, photon energy spectra are varied by transmitting through a multileaf collimator (MLC) and scattered photons in a medium. However, these effects on the depth scaling and the fluence scaling have not been clarified yet. In particular the depth scaling factor is indispensable in determining the fluence scaling factor.

The purpose of this study is to clarify effect of spectral variation on the depth scaling and to provide an accurate scaling method for IMRT beams. For this purpose, variations of photon energy spectra were obtained using the EGS Monte Carlo simulation. The depth scaling factors for commercially available solid phantoms were determined from effective mass attenuation coefficients using the photon energy spectra. The results clarified effect of spectral variation on the depth scaling.

*Corresponding author: Phone: +81(3)3819-1211,
Fax: +81(3)3819-1406,
E-mail: fujita-yukio@hs.tmu.ac.jp
[1]Graduate School of Human Health Sciences, Tokyo Metropolitan University, Higashiogu 7-2-10, Arakawaku, Tokyo 116-8551, Japan; [2]Chiba Cancer Center, Nitonachou 666-2, Chuouku, Chiba 260-8717, Japan.
doi:10.1269/jrr.10058

METHODS AND MATERIAL

Solid phantoms

In this study, as commercially available solid phantoms, WT1 (GAMMEX RMI, Wisconsin, USA), 457-CTG (GAMMEX RMI, Wisconsin, USA), RW3 (PTW, Freiburg, Germany), MixDP,[4] WE211 (Kyoto Kagaku, Kyoto, Japan), WE211R (Kyoto Kagaku, Kyoto, Japan), Plastic Water (CIRS, Virginia, USA), Plastic Water DT (CIRS, Virginia, USA), Virtual Water (Med-Cal, Wisconsin, USA), polystyrene, polymethyl methacrylate (PMMA) and acrylonitrile butadiene styrene (ABS) were evaluated. The elemental compositions, physical densities, electron densities and effective atomic numbers are summarized in Table 1.[2,5–7] The electron density ρ_e [g^{-1}] was calculated by,

$$\rho_e = \sum_i \frac{N_A w_i Z_i}{A_i} \quad (1)$$

where N_A is the Avogadro constant, w_i is fraction by weight, Z_i is atomic number and A_i is molar mass of i-th element, respectively. The effective atomic number Z_{eff} for the pair production was calculated as follows.[8]

$$Z_{eff} = \sum_i w_i Z_i \quad (2)$$

Depth scaling for photon beam

When monoenergetic photons with an incident fluence Φ_0 penetrate a layer with a mass attenuation coefficient μ/ρ and area density z, fluence behind the layer Φ is given by the following exponential attenuation law.

$$\frac{\Phi}{\Phi_0} = \exp[-(\mu/\rho)z] \quad (3)$$

If the ratio of photon fluence was equal at z_w in water and z_{pl} in a solid phantom, next relation will be established.

$$z_w = z_{pl}\frac{(\mu/\rho)_{pl}}{(\mu/\rho)_w} = z_{pl}(\mu/\rho)_{pl,w} \quad (4)$$

The term of $(\mu/\rho)_{pl,w}$ is redefined as the depth scaling factor c_{pl}. Thus, z_w can be determined by following equation.

$$z_w = c_{pl} z_{pl} \quad (5)$$

Calculation of depth scaling factor c_{pl} for megavoltage photon beam

Megavoltage photon beam produced by linear accelerator (linac) has a continuous energy spectrum, consequently, an effective mass attenuation coefficient is suitable for the depth scaling. The effective mass attenuation coefficient $\bar{\mu}/\rho$ can be obtained from a depth dose distribution such as

Table 1. The elemental compositions, physical densities, electron densities and relative electron densities for solid phantoms.[2,5–7]

Elements	Water	WT1	457-CTG	RW3	MixDP	WE211	WE211R	Plastic Water	Plastic Water DT	Virtual Water	Polystyrene	PMMA	ABS [a]
H	0.1119	0.0810	0.0810	0.0759	0.1277	0.0821	0.0838	0.0779	0.0740	0.0770	0.0774	0.0805	0.0810
B									0.0226				
C		0.6720	0.6720	0.9041	0.7682	0.6633	0.6738	0.5982	0.4670	0.6874	0.9226	0.5998	0.8490
N		0.0240	0.0240			0.0221	0.0219	0.0178	0.0156	0.0227			0.0700
O	0.8881	0.1990	0.1990	0.0080	0.0511	0.2065	0.1953	0.2357	0.3352	0.1886		0.3196	
Mg					0.0386				0.0688				
Al									0.0140				
Cl		0.0010	0.0010			0.0040	0.0024	0.0023	0.0024	0.0013			
Ca		0.0230	0.0230			0.0220	0.0228	0.0676		0.0231			
Ti				0.0120	0.0144								
ρ [g cm^{-3}]	0.998 [b]	1.020	1.043	1.045	1.000	1.018	1.018	1.030	1.039	1.030	1.060	1.190	1.050
ρ_e [$\times 10^{23}$ g^{-1}]	3.343	3.249	3.249	3.231	3.382	3.252	3.257	3.238	3.218	3.237	3.238	3.248	3.249
$(\rho_e)_{pl,w}$		0.972	0.972	0.966	1.012	0.973	0.974	0.969	0.963	0.968	0.969	0.972	0.972
Z_{eff} [c]	7.22	6.35	6.35	5.83	6.38	6.34	7.07	6.83	6.83	6.35	5.61	6.24	5.67

[a] Private letter given by Taisei Medical.
[b] The density for pure water at 22.0°C.
[c] The effective atomic number for pair production.

tissue-phantom ratio (TPR). The *TPR* for field size A and depth z can be expressed by following equation approximately.

$$TPR(z, A) = \exp\left[-(\bar{\mu}/\rho)(z - z_{ref})\right] \quad (6)$$

where z_{ref} is reference depth of TPR data. The reference depth is used for normalization of the TPR data. Thus, $\bar{\mu}/\rho$ can be determined by exponential approximation of TPR data.

However, to investigate influence of spectral variation for the depth scaling factor in detail, the $\bar{\mu}/\rho$ for several phantom materials were determined from photon energy spectra in this study. The $\bar{\mu}/\rho$ was calculated by,

$$\bar{\mu}/\rho = \frac{\int_{E_{min}}^{E_{max}} \Psi(E)[\mu(E)/\rho]dE}{\int_{E_{min}}^{E_{max}} \Psi(E)dE} \quad (7)$$

where $\Psi(E)$ is the differential energy fluence and $\mu(E)/\rho$ is the mass attenuation coefficient at photon energy E.[9] The photon energy spectra were determined by Monte Carlo methods as described in the next sub-section. The depth scaling factors were determined by following equation.

$$c_{pl} = \frac{(\bar{\mu}/\rho)_{pl}}{(\bar{\mu}/\rho)_{w}} \quad (8)$$

Monte Carlo simulation

Simulation of medical linear accelerator

The BEAMnrc code[10] was used to simulate a photon beam of Varian Clinac equipped with the Millennium 120 MLC (Varian Medical Systems, Palo Alto, CA). The geometrical data and material specifications were provided by the manufacturer. The accelerator head consists of several structures such as a target, primary collimator, vacuum window, flattening filter, secondly collimator and MLC. The MLC is composed of 80 inner leaves and 40 outer leaves whose projected width is 0.5 cm or 1.0 cm at the isocenter, respectively. The MLC was modeled by using the DYNVMLC component module.[10,11] The leaves are made of a tungsten alloy whose physical density ranges from 17.0 to 18.5 g cm^{-3} depending on the alloy composition and leaf manufacturing.[12] The density was adjusted by comparison between measured and calculated MLC transmission factor and 17.7 g cm^{-3} was employed in this report.

In this study, nominal photon energies of 4, 6, 10 and 15 MV were simulated. The initial electron energy and special distributions on the target were adjusted by comparing calculated and measured central axis depth dose and off-axis ratio in water.[13,14]

Calculation of photon energy spectra in phantom

The FLURZnrc code[15] was used to calculate photon spectra in a phantom. A phantom of height 30.0 cm and radius 20.0 cm was used for all simulation conditions. For sampling photon energy, cylindrical volume with height 0.2 cm and radius 0.2 cm were employed. The distance from source to the sampling region was fixed at 100 cm. The simulations were repeated until to get a statistical uncertainty of less than 1.0%. To clarify photon energy dependency of the depth scaling factor, photon energy spectra in each phantom for several photon energies, several depths and various field sizes were simulated.

For IMRT beams, the non-uniform fluence distribution is delivered by combining multi-segmental MLC field or sweeping MLC field. The variation of photon energy spectrum depends on the contribution of photons transmitted through the MLC. Namely completely blocked field by the MLC (blocked field) may show maximum variation of energy spectrum and maximum difference of the depth scaling factor is also expected. Therefore, the photon energy spectrum for the blocked field was also simulated.

RESULTS AND DISCUSSIONS

Photon energy dependence

The depth scaling factors for several photon energies and the relative electron densities are tabulated in Table 2. The depth scaling factors were determined from photon energy spectra at 10 cm depth with a 10 cm × 10 cm open field. For 4 MV and 6 MV, the depth scaling factors were almost equal to the relative electron density. However, for 10 MV and 15 MV, the depth scaling factors were varied from the relative electron density, except the Plastic Water. This is because the contribution of the pair-production is increased as photon energy increase. Figure 1 shows Compton and pair-production mass attenuation coefficients for the solid phantoms. These data were calculated by NIST's XCOM program.[16] The Compton mass attenuation coefficient is proportional to electron density and electron densities of solid phantoms are designed to be almost equal to water as shown in Table 1. Therefore, the Compton mass attenuation coefficients of the solid phantoms are equal to water as shown in Fig. 1-(a). In contrast, as shown in Fig. 1-(b), the pair-production mass attenuation coefficient of the solid phantom is different from water because of difference of the Z_{eff}. In particular, the depth scaling factors for the RW3, MixDP, polystyrene, PMMA and ABS showed significant variations from the relative electron density. Above all, the polystyrene showed lager difference between the depth scaling factor and relative electron density than the others. When the z_{pl} is calculated from equitation (5), the difference becomes 2.0 mm at 10 cm depth. By contrast, the Plastic Water had a constant depth scaling factor even though photon energy increases because it has the same pair-production and Compton mass attenuation coefficient as water.

Therefore, for solid phantoms which have a large difference in the Z_{eff}, the depth scaling factor should be deter-